Inorganica Chimica Acta, *125* (1986) 173–182

Spectroscopic Studies of Metal Complexes Containing π-Delocalized Sulfur Ligands. The Pre-Resonance Raman Spectra of the Antitumor Agent 2-Formylpyridine Thiosemicarbazone and Its Cu(II) and Zn(II) Complexes

HELOISA BERALDO

Département de Recherches Physiques, Université Pierre et Marie Curie, LA no. 71, 75230 Paris, France

and LUCIA TOSI

Departamento de Química, Universidade Federal de Minas Gerais, 30161, Belo Horizonte, Brazil

(Received May 20, 1986)

Abstract

The pre-resonance Raman spectra of 2-formylpyridine thiosemicarbazone have been measured at three pH values corresponding to the fully protonated (H_2FPT^+), half protonated (HFPT) and deprotonated (FPT^-) forms of the ligand. Assignments of the vibrations coupled with the $\pi \rightarrow \pi^*$ transition have been made by comparison with the spectrum of the deuterated form (DFPT). The pre-resonance Raman spectra of the Zn(II) and Cu(II) complexes, $[ZnFPT]^+$, $[CuFPT]^+$ and $[CuHFPT]^{2+}$, have also been measured. The spectral pattern of the Cu(II) complexes shows resonance enhancement of vibrations coupled with the $\pi \rightarrow \pi^*$, as well as with the ligand to metal charge transfer transitions. In addition, it is consistent with coordination through thiolate sulfur in $[CuFPT]^+$ and thione sulfur in $[CuHFPT]^{2+}$.

Introduction

In recent years transition metal complexes of the tridentate ligand 2-formylpyridine thiosemicarbazone (FPT) has been the subject of extensive investigation owing to their neoplasic and citotoxic activity. In a pioneering study French and coworkers showed that the conjugated N–N–S tridentate ligating structure and the need for a heterocyclic nitrogen are both prerequisite for carcinostatic activity [1–3]. In addition, several studies support the conclusion that the active form of the drug is its Fe(II) complex which causes marked inhibition of DNA synthesis, the principal site of cellular reaction being the enzyme ribonucleoside diphosphate reductase, an obligatory enzyme in the DNA synthetic pathway [4]. More recently it has been demonstrated that the Cu(II) complex of FPT has *in vitro* citotoxic effects against Erlich cells [5–7].

The tridentate ligand FPT is able to form 1:1 tetragonal metal complexes with Cu(II) and Zn(II) and 1:2 octahedral complexes with Fe(II), Fe(III) and Ni(II). In the first case the complexes are square planar, the fourth position being occupied by a second ligand (Fig. 1(a)). In the latter, two ligands are tridentately bound to the metal in two orthogonal planes (Fig. 1(b)). In addition, as in the case of its parent compound thiosemicarbazide, metal binding either through thiolate or thione sulfur are possible.

In acid media, Cu(II) forms two well defined complexes. The first is fully formed at pH $\geqslant$ 6.7 and the second at pH $\simeq$ 1.0. Petering and coworkers [8–9] have determined the formation constant of the first in aqueous solution assigning to it the structure of Fig. 1(a) with binding through thiolate sulfur and an oxygen of a water molecule in the fourth corner. For the second complex they assumed identical coordination and protonation at the exocyclic $N(4')H_2$ group.

In a previous report we presented a resonance Raman study on a bis-thiosemicarbazonato complex of Cu(II) (CuKTS) in aqueous solution. At low pH the ligand is protonated at the N(2′) level and the metal is bound through thione sulfur forming the cation $[CuH_2KTS]^{2+}$. At higher pH deprotonation takes place at N(2′) in which case the metal is coordinated to the thiolate sulfur. Protonation at the N(2′) centre of the thiosemicarbazide ring is responsible for substantial Raman frequency shifts in the resonance Raman spectra of $[CuH_2KTS]^{2+}$ as compared with that of CuKTS. The spectral changes reflect the increased double bond character of the C=S bond which gives rise to less conjugation of the double bonded C=N groups [10].

These results prompted us to initiate a resonance Raman study of the Cu(II) complexes of FPT in order to test Petering and coworkers assumption. In this report we present resonance Raman measurements of the ligand in acid, neutral, and alkaline

0020-1693/86/$3.50

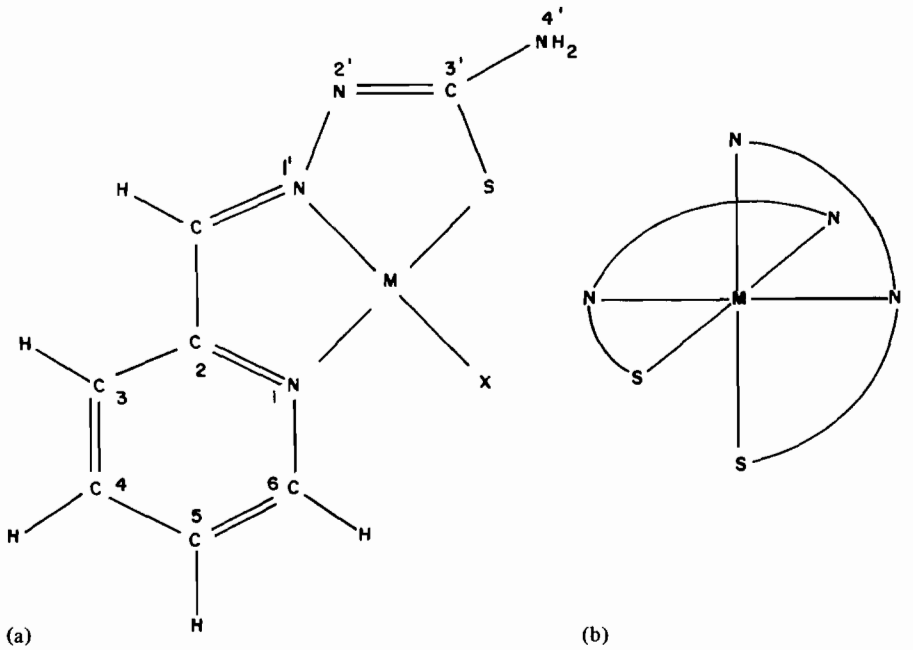

Fig. 1. General structure of (a) square planar and (b) octahedral complexes of 2-formylpyridine thiosemicarbazone.

media, and of both Cu(II) and Zn(II) complexes, which enable a better insight on metal–ligand binding and on the site of protonation.

Experimental

2-Formylpyridine thiosemicarbazone (FPT) was obtained by the method of Anderson *et al.* [11]. The Cu(II) complex in the solid state was prepared by the method of Antholine *et al.* [5]. The Zn(II) complex was obtained by titration of the ligand in aqueous solution containing 1.0% DMSO with Zn(II) ions [8].

All the chemicals were of the best reagent grade. Demineralized distilled water, previously freed of organic contaminants was used throughout.

Raman spectra were measured on a Coderg D 800 spectrometer equipped with holographic gratings. The detector used a DC amplifier and a cooled RCA C31034 PM tube. The exciting lines were those of an Ar^+ Spectra Physics laser. Raman intensities were measured relative to the intensity of the $\nu_1(ClO_4^-$ or $SO_4^{2-})$ band used as internal standard. The excitation profiles are reported as the ratio of the peak height of a given band to that of the internal standard. Intensity measurements using the area under the bands gave similar results. The ratios were corrected for sample absorption, instrumental spectral response and scattered radiation frequency.

Absorption measurements were made on a Cary 219 spectrometer.

Results and Discussion

The Electronic and Raman Spectra of FPT

The proton dissociation constants of FPT may be defined by the following equilibria:

$$H_2FPT^+ \overset{K_1}{\rightleftharpoons} HFPT + H^+$$

$$HFPT \overset{K_2}{\rightleftharpoons} FPT^- + H^+$$

The first corresponds to deprotonation at the pyridine nitrogen and the second at the thiolate group.

In Figs. 2 and 3 are represented the absorption spectra of an aqueous solution of FPT in the presence of 0.5% DMSO at various pH. At low pH, the spectra of Fig. 2 display two bands lying at 348 nm (ϵ_{max} = 20 500 M^{-1} cm^{-1}) and 268 nm (ϵ_{max} = 7700 M^{-1} cm^{-1}) arising from $\pi \rightarrow \pi^*$ transitions. At pH higher than 3 both bands coalesce giving rise to a broad absorption at 315 nm (ϵ_{max} = 24 000 M^{-1} cm^{-1}) with a shoulder at $\simeq$ 270 nm. There are two isosbestic points at 276 and 330 nm. This spectrum remains unchanged up to approximately pH 10 when the maximum shifts again to lower energy as pH increases (Fig. 3). At pH 13 the spectra level off and are characterized by a broad and assymetric band at 345 nm (ϵ_{max} = 18 600 M^{-1} cm^{-1}), with two isosbestic points at 328 and 250 nm. Using these spectral data the values of $pK_1 = 3.61 \pm 0.2$ and $pK_2 = 11.50 \pm 0.2$ are calculated which compare

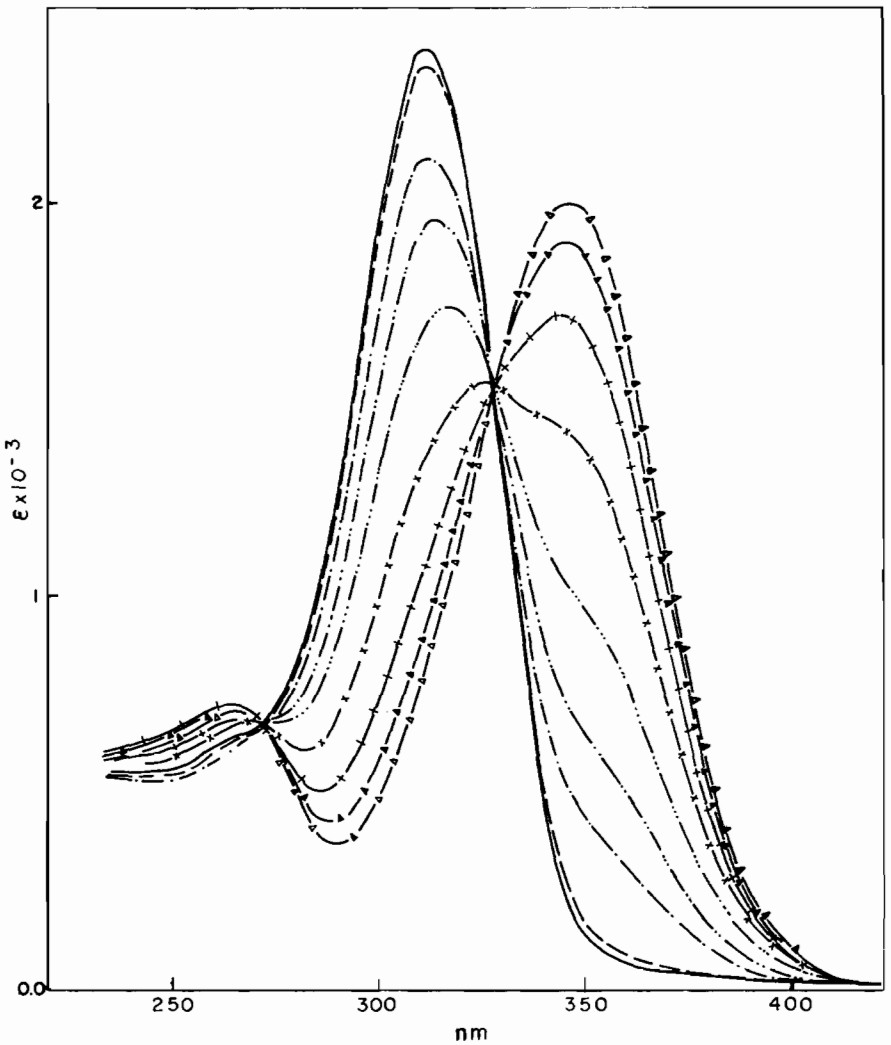

Fig. 2. Spectrophotometric titration curves of HFPT with $HClO_4$ in aqueous solution containing 0.5% DMSO. [HFPT] = 6.35 × 10^{-4} M. —— pH 6.73, - - - pH 5.35, - · - pH 4.31, - · · - pH 4.02, - · · · - pH 3.68; - × - pH 3.27, - + - pH 2.84, - ▲ - pH 2.35, - △ - pH 1.55, - ○ - pH 1.14.

with that obtained by Knight *et al.* (3.60 and 10.97 respectively) [9].

The spectral pattern observed at high pH does not differ esssentially from that in acid media since the broad band at 345 nm can be decomposed in one stronger at ~350 nm and another much weaker at ~310 nm. This spectral behavior can be accounted for by assuming that Z–E (*syn–anti*) isomerization is occurring.

As shown in Scheme 1, at pH above 6.5 and up to pH 10, HFPT is assumed to be in the Z configuration which is stabilized by hydrogen bonding between the proton at N(2′) and the pyridine N(1) nitrogen (configuration **II**). In acid media, when pyridine is protonated, such a structure (**II**) becomes very unfavorable because of steric hindrance, the most stable form being the E configuration (**I**). At higher pH, when the pyridine nitrogen and the thiolate group are both deprotonated, configuration Z (**III′**) and E (**III**) should be, in principle, equally stable. However, the similarity between H_2FPT and FPT^- spectra suggests that the latter adopts the E configuration. The **III** → **III′** isomerization is slow; one must wait 10 to 15 min to attain equilibrium in pH readings.

The pK that are actually measured by spectrometric titrations are those corresponding to the equilibria:

$$\mathbf{I} \overset{K_1}{\rightleftharpoons} \mathbf{II}$$

$$\mathbf{II} \overset{K_2}{\rightleftharpoons} \mathbf{III}$$

The pre-resonance Raman (PRR) spectra of H_2-FPT at pH < 1 and of FPT at pH 13 are illustrated

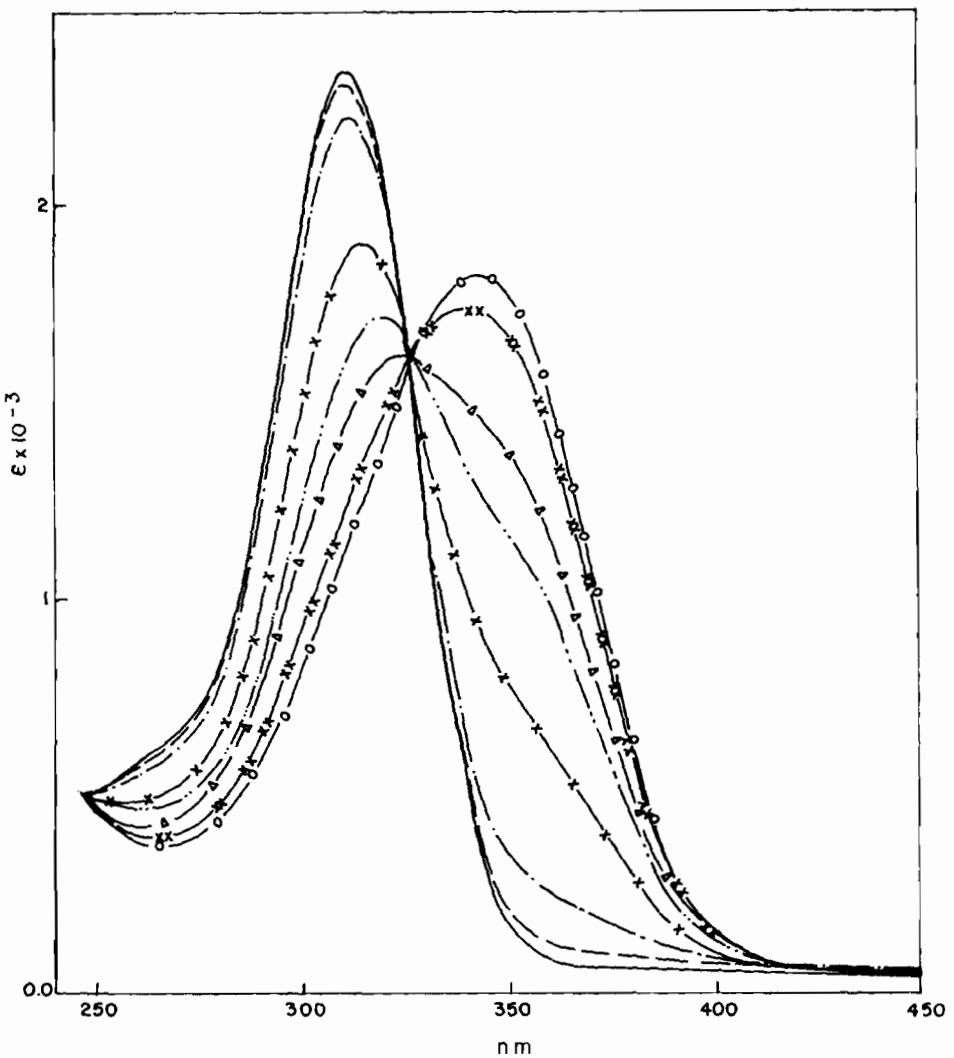

Fig. 3. Spectrophotometric titration curves of HFPT with NaOH in aqueous solution containing 0.5% DMSO. [HFPT] = 6.35 × 10^{-4} M. —— pH 7.23, - - - pH 9.69, - · - pH 10.45, - × - pH 11.46, - · · - pH 11.94, - △ - pH 12.38, - ×× - pH 13.02, - ○ - pH 13.81.

in Fig. 4. In Fig. 5 are represented the PRR spectra of HFPT at pH 6.52 and that of the deuterated form at pH 6.92. Wave numbers and assignments are summarized in Table I. The bands lying above 1500 cm^{-1} do not shift upon deuteration indicating that the $N(4')H_2$ deformation mode, which must be found in this region, is not enhanced by resonance. In other words: the $N(4')H_2$ group is not involved in the π-delocalized system giving rise to the electronic transitions at 315 and 345 nm. Hence, only skeletal vibrations, ν_{CC} and ν_{CN} are expected to be observed. The spectra of the three species exhibit three very strong bands above 1550 cm^{-1}, one of which is appreciably shifted by protonation of pyridine and to a less extent by disappearance of hydrogen bonding between the pyridine nitrogen and the N(2') proton; *i.e.* from 1620 cm^{-1} in the spectrum of HFPT to 1637 cm^{-1} in that of H_2FPT^+ and to 1610 cm^{-1} in that of FPT^- (see Table I). So, it may be safely assigned to the 8a, ν_{CC} stretching mode, that is found at 1580 cm^{-1} in the Raman spectrum of pyridine [12].

The Raman spectrum of thiosemicarbazide presents two bands at 1530 and 1499 cm^{-1} assigned mainly to the ν_{CN} and amide II ($\nu_{CN} + \delta_{NH}$) modes respectively [13]. We propose a similar assignment for the two doublets at 1570–1600 cm^{-1} and 1445–1480 cm^{-1}. In fact, the intensity of the latter appears to decrease in the spectrum of the deuterated form of Fig. 5, while two new bands are noticeable at 1414 and 1358 cm^{-1}, confirming their assignment to the amide II mode (see Fig. 5).

In addition, there are two peaks at 1115 and 1097 cm^{-1} in the spectrum of HFPT that practically disappear in that of the deuterated form whereas two new bands are noticeable as shoulders of the

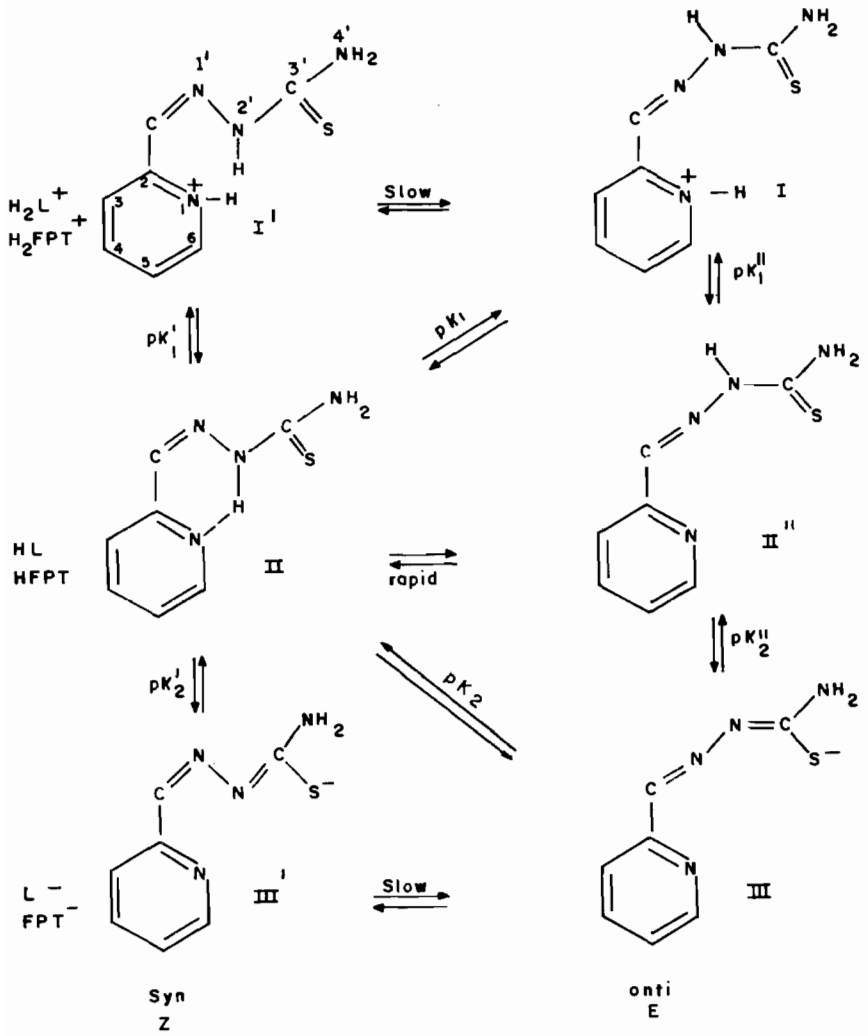

Scheme 1.

two DMSO bands at 1015 and 935 cm^{-1}: one shoulder is observed at the high frequency side of the first and the other at the low frequency side of the second (see Fig. 5 and Table I). One expects to find in this region the CS stretching vibration. It appears in the 1150–1400 cm^{-1} region in the infrared spectra of thioureas and this rather wide range is attributed to varying degrees of coupling with other vibrations [2]. Furthermore, it has been shown that the CS stretching mode of thiosemicarbazide is distributed among three Raman bands at 1010, 808 and 508 cm^{-1} that shift respectively to 924, 710 and 435 cm^{-1} upon deuteration. The band at 808 cm^{-1} is attributed mainly to the ν_{CS} mode whereas the $N'(4)H_2$ rocking mode contributes to the peak at 1010 cm^{-1} and the NCN deformation to that at 508 cm^{-1} [14]. We thus propose to assign the bands at 1115 and 1097 cm^{-1} in the spectra of HFPT to the CS stretch coupled with the $N(4')H_2$ rocking mode. It is worth noting that as pyridine protonates, these bands shift to 1135 and 1057 cm^{-1} respectively (Fig. 4) and coalesce in a band at 1102 cm^{-1} when the CS group is in the thiolate form (see Fig. 4 and Table I). This result corroborates the assumption that the ν_{CS} stretch is coupled to other modes in varying degrees. It suggests that there must be some contribution from the N(2′)H deformation mode since, independently of configuration, in passing from HFPT to FPT^-, N(2′)H deprotonates and thione substitutes for thiolate (see structures **II** and **III** or **III′** of Scheme 1).

There is another band in this spectral region which does not shift upon deuteration and is only slightly perturbed by protonation of pyridine. It lies at 1010 cm^{-1} in the spectrum of H_2FPT^+, at 1007 cm^{-1} in that of HFPT and at 1005 cm^{-1} in that of FPT^- (see Figs. 4 and 5, and Table I). It may be assigned to the ν_1 totally symmetric mode of pyridine which is observed at 995 cm^{-1} in the Raman spectra of this compound [12].

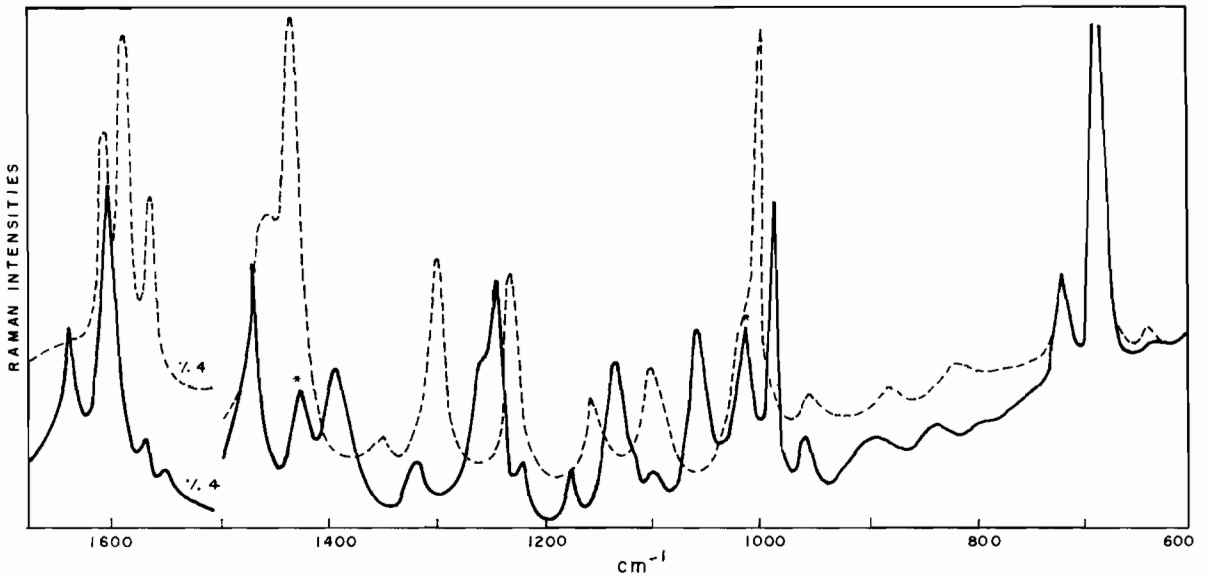

Fig. 4. Pre-resonance Raman spectra of H_2FPT^+ (pH ~ 0.7) ——, and FPT^- (pH = 13.0) - - - in aqueous solution containing 0.5% DMSO using the 457.9 nm Ar^+ exciting radiation, 80 mW, slit width = 5 cm^{-1}, scanning speed 50 cm^{-1}/min, time constant 0.5 s. $[H_2FPT] = [FPT^-] = 1.52 \times 10^{-3}$ M. The asterisks indicate the DMSO bands.

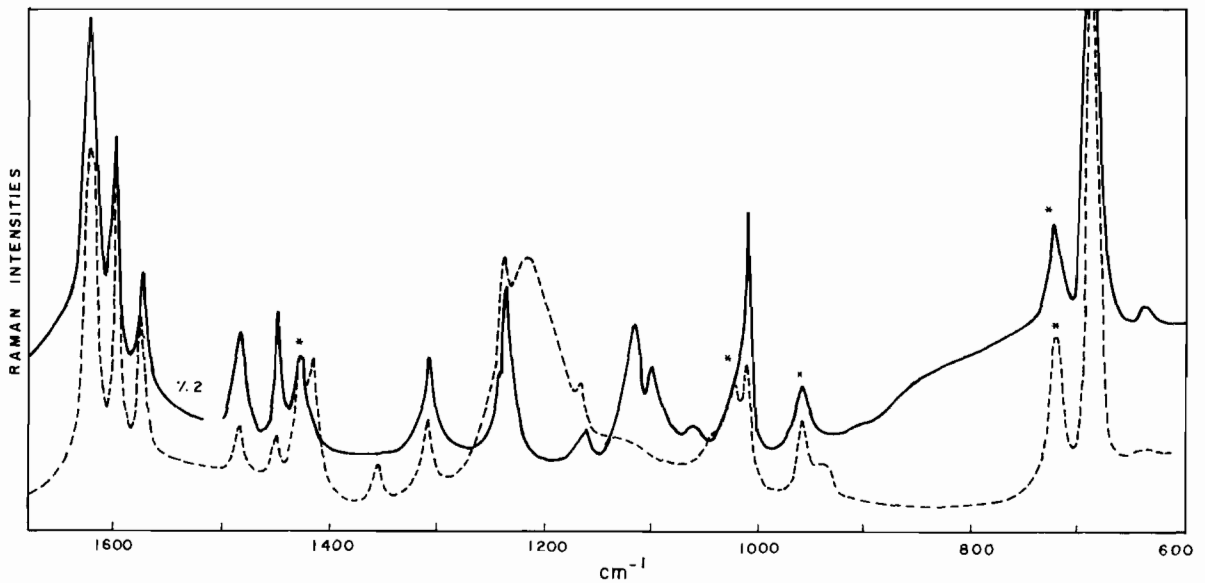

Fig. 5. Pre-resonance Raman spectra of HFPT (pH = 6.52) ——, and DFPT (pH = 6.92) - - - in H_2O and D_2O solution respectively containing 0.5% DMSO using the 457.9 nm Ar^+ exciting radiation, power 80 mW, slit width = 5 cm^{-1}, scanning speed 50 cm^{-1}/min, time constant 0.5 s. [HFPT] = [DFPT] = 1.26×10^{-3} M. The asterisks indicate the DMSO bands.

The very weak bands at 890 and 837 cm^{-1} in the spectrum of HFPT that shift to 880 and 817 cm^{-1} respectively in the spectrum of the deprotonated form may be ascribed to the NCN deformation coupled to ν_{CS}. However, they are not observed in the spectrum of the deuterated form although they should shift upon deuteration [14]. The other very weak bands at lower frequency are attributed to pyridine and NCN deformation modes (see Table I).

The Electronic and Pre-resonance Raman Spectra of Zn(II) and Cu(II) Complexes of FPT

As shown by Antholine *et al.* [8] using spectrometric titration curves of HFPT with Zn(II), when complexation occurs, the ligand absorption at 315 nm is split into two others at 363 nm (ϵ = 14 200 M^{-1} cm^{-1}) and 276 nm (ϵ = 12 200 M^{-1} cm^{-1}) which are characteristic of the complex. Two isosbestic points are present at 280 and 333 nm.

TABLE I. Resonance Raman Wave Numbers and Assignments[a]

H_2FPT^+ pH ≃0.7[b]	HFPT pH 6.52	DFPT pH 6.92	FPT^- pH 13.0	$[ZnFPT]^+$ pH 6.50	$[CuFPT]^+$ pH 6.57	$[CuHFPT]^{2+}$ pH ≃0.5[b]	Assignment
1637vs	1621vs	1620vs	1610vs	1619s	1618s	1630vs	ν_{CC} py (8a)
1602vs	1600s	1598s	1592vs	1603sh	1598m	1600vw	ν_{CN}
1570w	1572m	1575m	1568vs	1570s	1573vs	1575s	
1550vw							
1470m	1480w	1482vw	1460s	1480w	1485w	1485m	$\nu_{CN} + \delta N(2')H$
1447w	1445w	1445vw	1432vs	1437sh	1450s	1450s	
1425w	1425w	1425w		1425m	1425sh		DMSO
		1414w					$\nu_{CN} + \delta N(2')D$
1392w					1395w	1395vw	$\nu_{NN} + \nu CN$
		1358w					$\nu_{CN} + \delta N(2')D$
1317w	1308w	1307w	1300s	1310w	1310w	1310w	$\nu_{NN} + \nu_{CN}$
1260sh					1275w		$\nu_{NN} + \nu_{CN}$
1246m							
1220w	1212m	1225w	1232s	1235w	1235m	1235w	
		1205sh			1200w		D_2O
1175vw				1175m	1180s	1190s	$\nu_{NN} + \nu_{CN}$
	1162vw	1165w		1160m	1165s	1165w	
1135m							$\nu_{CS} + r_{N(4')H_2}$
1100vw	1115m	1115vw	1102m	1115w	1115w	1115w	
1057m	1097w			1095w		1060s	ν_{CS}
		1035sh					$\nu_{CS} + r_{N(4')D_2}$
	1015w	1015w	1015sh				DMSO
1016m	1007m	1009m	1005vs	1022m	1028s	1028m	ν_1 py
988w						986s	$\nu_1 SO_4^-$
955w	955w	955w	955w	955w			DMSO
					936vs		$\nu_1 ClO_4^-$
		935sh					ν_{CS}
	890vw		880vw	890vw	890vw	892vw	$\delta_{NCN} + \nu_{CS}$
	837vw			842vw	850vw	850vw	
			817vw	800w		750w	
715w	715w	715w	715w	715w			DMSO
					685m	682vw	ν_{CS}
680vs	680vs	680vs	680vs	680vs			DMSO
					655m	650vw	$\nu_{CS} + \delta$ring
630vw	632vw	630vw	635vw	640vw			6b py
				625vw	632m	630vw	6a py + δring
595vw						600vw	6a py
				540vw	505vw		δring
	460w				465w	450w	
415vw							
					300m	310vw	ν_{MS}

[a]s, strong; vs, very strong; w, weak; vw, very weak, b, broad; sh, shoulder. [b]pH below 1 are estimated.

The absorption spectrum of the acetate salt of $[Cu(II)FPT]^+$ in aqueous solution exhibits three bands at 280 nm (ϵ = 14 750 M^{-1} cm^{-1}), 320 nm (ϵ = 11 000 M^{-1} cm^{-1}) and 384 nm (ϵ = 9400 M^{-1} cm^{-1}). This spectrum is similar to that obtained by Antholine *et al.* by spectrometric titration of HFPT

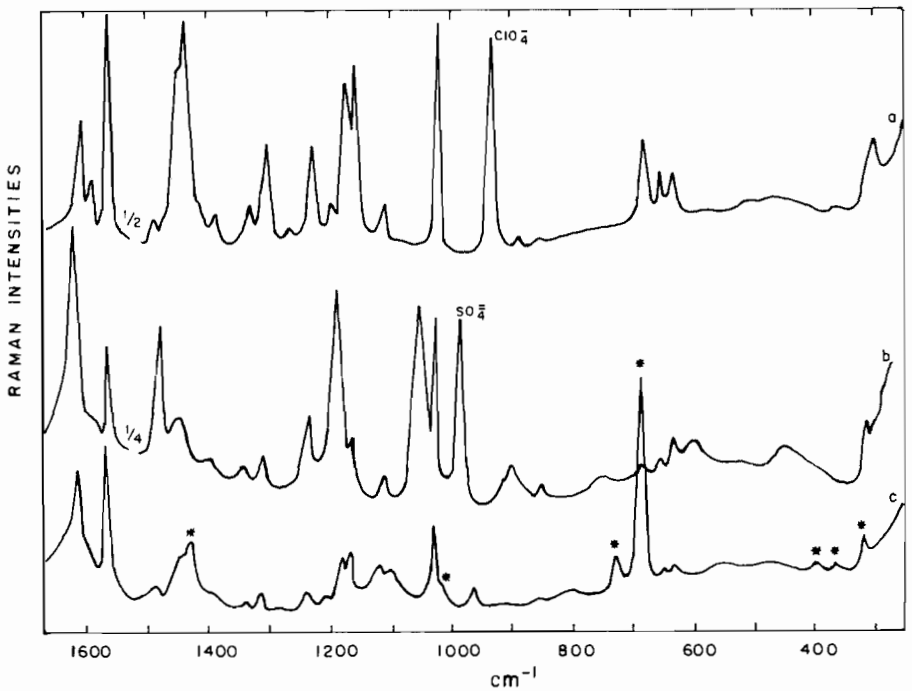

Fig. 6. PRR spectra: curve a, $[CuFPT]^+$ at pH ~ 0.5 in aqueous solution; curve b, $[CuHFPT]^{2+}$ at pH 6.57 in aqueous solution; curve c, $[ZnFPT]^+$ at pH 6.52 in aqueous solution containing 1% DMSO. Spectra were obtained using the 454.5 nm Ar^+ exciting radiation. Experimental conditions: laser power: 80 mW, slit width = 5 cm^{-1}, scanning speed = 50 cm^{-1}/min, time constant 0.5 s. $[CuFPT]^+ = [CuHFPT]^{2+} = 1.68 \times 10^{-3}$ M. The asterisks indicate the DMSO bands.

with Cu(II), which they assigned to the monomeric form of the complex with a water molecule at the fourth corner [8]. As shown by these authors, when the complex is titrated with acid, a new species appears, $[CuHFPT]^{2+}$, displaying absorption bands at 264 nm (ϵ = 11 000 M^{-1} cm^{-1}), 306 nm (ϵ = 16 400 M^{-1} cm^{-1}) and a shoulder at 344 nm ($\epsilon \simeq$ 7200 M^{-1} cm^{-1}) and three isosbestic points are observed at 268, 292 and 324 nm [8]. A deprotonation constant is detected with pK = 2.40 [9].

As observed previously, in the case of $[Fe(II)(FPT)_2]$ [15], formation of the Zn(II) and Cu(II) complexes are thus characterized by the splitting of the ligand absorptions at 315 nm in two others. However, one additional intense band appears upon complexation in the spectra of both Cu(II) and the Fe(II) complexes, at 384, 344 and 610 nm respectively [8, 15] that is not observed in that of the Zn(II) compound [8]. As in the case of the Fe(II) complex [15], we assign this new band to a ligand-to-metal charge transfer transition (LMCT). Obviously, since Zn(II) has a closed d shell, such transition is precluded.

The PRR spectra of $[CuFPT]^+$ and $[CuHFPT]^{2+}$ in aqueous solution are illustrated in Fig. 6, curves a and b respectively. Curve c represents the PRR spectrum of $[ZnFPT]^+$ in aqueous solution containing 1% DMSO. Wave numbers are summarized in Table I. In the region above 1160 cm^{-1}, characteristic of ν_{CC}, ν_{CN} and ν_{NN} skeletal modes, there is practically no change in frequencies as compared to those of the HFPT spectrum, although some differences in relative intensities are noticeable. The only exception corresponds to the skeletal 8a pyridine mode that shifts from 1610 cm^{-1} in the spectrum of HFPT to 1630 cm^{-1} in that of $[Cu(HFPT)]^{2+}$ (see Fig. 6 and Table I).

On the other hand, in the region below 1160 cm^{-1} some remarkable changes in the spectra of both Cu(II) complexes are noticeable. Thus, the band at 1097 cm^{-1}, disappears and four new bands are observed at 685, 655, 632 and 300 cm^{-1} in the spectrum of $[CuFPT]^+$. By protonation of this complex to give $[CuHFPT]^{2+}$ these bands decrease considerably in intensity, in particular the one at 685 cm^{-1}, and a strong band appears at 1060 cm^{-1}. In addition, the ν_1 pyridine breath mode shifts to higher frequencies (21 cm^{-1}) in the spectra of both complexes. An analogous shifting of this same band (15 cm^{-1}) is observed in the spectrum of $[ZnFPT]^+$, this being practically the only difference as far as frequencies are concerned, between the spectra of the Zn complex and that of HFPT.

These changes may be interpreted on the basis of our assignment of the 1097 cm^{-1} band mostly to the CS stretching mode since we expect its shifting to lower frequencies upon sulfur coordination to the metal as thiolate [15]. As we have shown above,

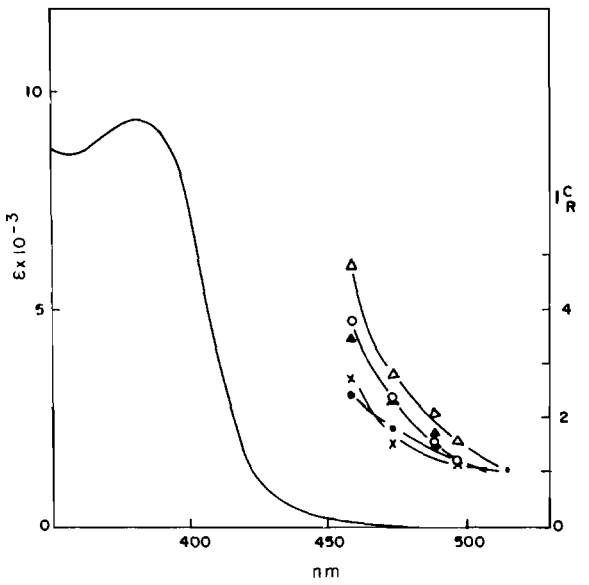

Fig. 7. Raman excitation profile of $[CuFPT]^+$ in aqueous solution, pH 6.57. —— Absorption spectrum. I_R^c are the corrected intensity ratios in arbitrary units. Principal Raman bands: (○) 300 cm^{-1}, (△) 685 ~ 655 > 635 cm^{-1}, (▲) 1450 cm^{-1}, (●) 1572 cm^{-1}, (X) 1618 ≃ 1028 cm^{-1}.

deuteration experiments indicate that both the 1097 and the 1115 cm^{-1} bands contain some contribution of the $N(4')H_2$ rocking and probably the $N(2')H$ deformation modes. However, upon complexation, only the band at 1097 cm^{-1} shifts to lower frequencies indicating that once thiolate is bound to the metal, the CS stretch is no more coupled with the $N(4')H_2$ rocking mode and shifts to lower frequencies. Consequently, we may safely assign the bands at 685, 655 and 632 cm^{-1} mainly to the CS stretching vibration of the thiolate bound to Cu(II) probably coupled with deformation ring modes. In addition, the CuS stretch may be associated with the band at 300 cm^{-1}.

The existence of one half-filled d orbital in Cu(II) as well as that of three lone pairs in thiolate may, in principle, result in three LMCT transitions in the spectra of $[CuFPT]^+$, one $\sigma(S) \rightarrow \sigma^*Cu(II)$ of higher energy and two $\pi(S) \rightarrow \sigma^*(Cu(II)$ of lower energy. If the transition involves a $\pi(S) \rightarrow \sigma^*Cu(II)$LMCT, one of the lone pair electrons of the sulfur should be brought onto the antibonding orbital of the metal and the CS bond length is expected to become longer in the excited state. In addition, the depopulation of the sulfur π orbital would lower the extent of conjugation with the π system including the bichelate and the pyridine ring. Therefore, the vibrations predominantly involved in the transition should be the CS, CC and CN stretches and ring deformations coupled with them. As the excitation profile of Fig. 7 shows, those are precisely the bands enhanced by resonance, the most enhanced being those at 685–635 and the one at 300 cm^{-1}. It is interesting to recall that we obtained a similar enhancement pattern and similar frequencies in the case of CuKTS, the RR spectrum of which showed three bands strongly enhanced by resonance lying at 714, 632 and 595 cm^{-1}. We assigned the first to pure ν_{CS} and the two others to ring deformations [10].

Thione sulfur is formed when protonation of the ligand, occurs at N(2′) in $[CuHFPT]^{2+}$ (configuration II′); it is less polarizable than thiolate sulfur and has only two lone pairs. So, there must be two LMCT transitions in the electronic spectrum of $[Cu(HFPT)]^{2+}$, one strongly allowed $\sigma(S) \rightarrow \sigma^*Cu(II)$ at higher energy and one $\pi(S) \rightarrow \sigma^*Cu(II)$ at lower energy. Both should occur at higher frequencies than those of $[CuFPT]^+$ [10, 16]. A shift of 40 nm, as indicated above [8], is quite plausible. In addition, one must expect an increase in the double bond character of the CS thione bond and consequently, a shifting of the CS stretching mode to higher frequencies. This, again, is what one observes in the spectrum of Fig. 6, curve b. The bands at 685–632 cm^{-1} decrease considerably in intensity and a band at 1060 cm^{-1} reappears *i.e.* practically at the same frequency observed in the spectrum of H_2FPT^+. An analogous behaviour was found in the spectra of CuKTS by protonation at N(2′) although the shift was only of 130 cm^{-1} instead of 375 cm^{-1} as in the present case [10].

In the spectrum of the Zn(II) complex, on the other hand, the band at 1115 cm^{-1} appears to decrease in intensity with respect to the 1097 cm^{-1} peak indicating that the CS stretching and the $N(4')$-H_2 rocking vibrations are still coupled (see Fig. 6(c)). As expected, there is no observable enhancement of any band below 900 cm^{-1} which could be attributed to the CS stretch, unless it is masked by the strong DMSO band at 680 cm^{-1}. As there is no LMCT transition, the spectrum of Fig. 6(c) corresponds, in fact, to the vibrations coupled with the $\pi \rightarrow \pi^*$ ligand transition at 363 cm^{-1}. The small differences observed in relative intensities and frequencies as compared with that of the ligand at pH 6.52 are due to the fact that the molecular orbitals involved in the transition are perturbed by complexation. A similar statement holds for the spectra of both Cu(II) complexes in the region above 1160 cm^{-1} which in this case must be the result of two preresonance phenomena: one corresponding to the enhancement of the vibrations coupled with the $\pi \rightarrow \pi^*$ transition (at 320 and 306 nm) and the other with the vibrations coupled to the $\pi(S) \rightarrow \sigma^*Cu(II)$ LMCT transition (at 384 and 344 nm). The considerable difference in band intensities between the a (or b) and c spectra in the $\nu_{C=C}$ and $\nu_{C=N}$ regions are consistent with this interpretation.

Finally, another interesting fact to note is the frequency of the 8a pyridine mode in the PRR

spectrum of $[Cu(HFPT)]^{2+}$ which compares with that observed in the spectrum of the ligand at pH < 1 (see Table I). The 1630 cm^{-1} band appears, in the spectrum of $[Cu(HFPT)]^{2+}$, at pH 1.5 whereas the band at 1060 cm^{-1} appears at pH 1.25. As we have stated above, $[Cu(HFPT)]^{2+}$ deprotonates with a $pK = 2.40$ whereas the pK_a of the pyridine nitrogen of H_2FPT is 3.60 [9]. So, it seems by no means improbable that protonation of pyridine nitrogen and of N(2′) occurs almost simultaneously. This assumption implies that the $[Cu(HFPT)]^{2+}$ complex is in fact a monochelate.

Further experiments are underway in order to test this latter suggestion.

Acknowledgements

We are indebted to Maria de Lourdes Anastácio Lima for technical assistance. H. Beraldo is grateful to CAPES (Brazil) for a fellowhip in D.R.P.

References

1 F. A. French and E. J. Blanz, Jr., *J. Med. Chem., 9*, 585 (1966).
2 E. J. Blanz, Jr., F. A. French, J. R. DoAmaral and D. A. French, *J. Med. Chem., 13*, 1124 (1970).
3 F. A. French, E. J. Blanz, Jr., S. C. Schaddix and R. W. Brockman, *J. Med. Chem., 17*, 172 (1974).
4 A. C. Sartorelli, K. C. Agrawal, A. S. Tsiftsoglou and E. C. Moore, in G. Weber (ed.), 'Advances in Enzyme Regulation', Vol 15,, Pergamon, New York, 1977, p. 117.
5 W. E. Antholine, J. M. Knight and D. H. Petering, *J. Med. Chem., 19*, 339 (1976).
6 L. A. Saryan, E. Ankel, C. Krishnamurti, D. H. Petering and H. Elford, *J. Med. Chem., 22*, 1218 (1979).
7 L. A. Saryan, K. Mailer, C. Krishnamurti, W. Antholine and D. H. Petering, *Biochem. Pharmacol., 30*, 1595 (1981).
8 W. E. Antholine, J. M. Knight and D. H. Petering, *Inorg. Chem., 16*, 569 (1977).
9 J. M. Knight, H. Whelan and D. H. Petering, *J. Inorg. Biochem., 11*, 327 (1979).
10 L. Tosi and A. Garnier-Suillerot, *J. Chem. Soc., Dalton Trans.*, 103 (1982).
11 F. L. Anderson, F. J. Duca and J. V. Scudi, *J. Am. Chem. Soc., 73*, 4967 (1951).
12 L. Corrsin, B. J. Fax and R. C. Lord, *J. Chem. Phys., 21*, 1170 (1953).
13 L. J. Bellamy, 'The Infrared Spectra of Complex Molecules', 3nd ed., Chapman and Hall, London, 1975.
14 G. Keresztury and M. P. Marzocchi, *Spectrochim. Acta, Part A, 31*, 275 (1975).
15 H. Beraldo and L. Tosi, *Inorg. Chim. Acta, 75*, 249 (1983).
16 M. G. M. Campbell, *Coord. Chem. Rev., 15*, 279 (1975).